Talanta 105 (2013) 255–261

Contents lists available at SciVerse ScienceDirect

Talanta

journal homepage: www.elsevier.com/locate/talanta

Superparamagnetic surface molecularly imprinted nanoparticles for sensitive solid-phase extraction of tramadol from urine samples

Tayyebeh Madrakian *, Abbas Afkhami, Hediye Mahmood-Kashani, Mazaher Ahmadi

Faculty of Chemistry, Bu-Ali Sina University, Hamedan, Iran

ARTICLE INFO

Article history:
Received 1 October 2012
Received in revised form
10 December 2012
Accepted 13 December 2012
Available online 31 December 2012

Keywords:
Molecularly imprinted polymer
Magnetic nanoparticles
Tramadol
Solid-phase extraction

ABSTRACT

A rapid, selective, sensitive and accurate method based on superparamagnetic molecularly imprinted polymer nanoparticles (MMIPNPs) was developed for the determination of tramadol (TRA) in human urine samples. The MMIPNPs were prepared by coating SiO_2–Fe_3O_4 nanoparticles with polyaminoimide homopolymer and TRA as the template. The prepared MMIPNPs adsorbent was characterized by TEM, FT-IR, XRD and magnetometry. TEM images show that the Fe_3O_4 nanoparticles are well-enwrapped by the SiO_2 shell and further by an MIP layer. The prepared magnetic adsorbent is well dispersed in water and can be easily separated magnetically from the medium after loading with the adsorbate. Various parameters affecting the extraction efficiency of the MMIPNPs have been evaluated. The extracted TRA could be easily desorbed with a mixture of methanol and acetic acid and determined spectrophotometrically at 272 nm. A linear dynamic range was established from 3.0 to 200.0 ng mL^{-1} of TAR and the limit of detection was found to be 1.5 ng mL^{-1}. The proposed method was successfully applied for the determination of TRA in human urine samples.

1. Introduction

Tramadol, (2-[(dimethylamino) methyl]-1-(3-methoxyphenyl) cyclohexanol), TRA, is a centrally acting analgesic, prescribed for the treatment of moderate to severe pain [1]. The Food and Drug Administration (FDA) approved TRA in 1995 for legal use in the United States. Impairing side effects of TRA include dizziness, confusion, light-headedness or fainting spells, drowsiness, seizures and respiratory depression [2]. After oral administration, TRA demonstrates 68% bioavailability, with peak serum concentrations reached within 2 h. The elimination kinetics can be described as 2-compartmental, with a half-life of 5.1 h for TRA and 9 h for the O-desmethyltramadol (its main metabolite) after a single oral dosage [3–5].

Several analytical methods have been reported for the determination of TRA and/or its metabolites in a variety of biological matrices. These methods include: HPLC with UV [6–9], fluorescence [9,10], or diode array detectors [11]; gas chromatography (GC) [12]; three-phase hollow fiber liquid-phase microextraction/GC-MS [13]; and MS [14–17]. Simultaneous quantification of TRA and its metabolites in brain tissue of mice and rats [18], saliva [19], urine [19,20], amniotic fluid [21] and plasma [22,23] have been reported using different analytical techniques.

Pertinent sample preparation is crucial for obtaining meaningful results from the analysis of real samples, since it is the most tedious and time-consuming step and a possible source of imprecision and inaccuracy of the overall analysis. Solid-phase extraction (SPE) is widely used for the extraction and preconcentration of analytes in various environmental, food and biological samples. It is the most popular clean-up technique due to factors such as convenience, cost, time saving and simplicity and it is the most accepted sample pretreatment method today [24,25]. At present, there are several types of sorbents for SPE, including normal-phase, reversed-phase, ionic, and other special sorbents. However, due to their unsatisfactory selectivity, these traditional sorbents usually cannot separate analytes efficiently in complex biological or environmental samples [26]. A relatively new development in the area of SPE is the use of molecularly imprinted polymers (MIPs) for the sample clean-up and development of selective and sensitive analytical methods [27–30]. MIPs are synthetic polymers possessing specific cavities designed for a target molecule and are synthesized by the polymerization of different components. In the most common preparation process, monomers form a complex with the desired template through covalent or non-covalent interactions and then joined by using a cross-linking agent. After removing the template by chemical reaction or extraction, binding sites are exposed which are complementary to the template in size, shape, and position of

* Corresponding author. Tel./fax: +98 811 8257407.
E-mail addresses: madrakian@basu.ac.ir, madrakian@gmail.com (T. Madrakian).

0039-9140/$ - see front matter © 2012 Elsevier B.V. All rights reserved.
http://dx.doi.org/10.1016/j.talanta.2012.12.039

the functional groups, and consequently allow its selective uptake [24]. MIPs are often referred to as artificial antibodies. Unlike antibodies, MIPs are stable to extremes of pH, organic solvents and temperature which allow more flexibility in the analytical methods [26,27]. The use of MIPs for SPE involves conventional SPE where the MIP is packed into columns or cartridges [31,32] and batch mode SPE in which the MIP is incubated with the sample [33]. A major advantage of MIP-based SPE, related to the high selectivity of the sorbent, is achievement of an efficient sample clean-up.

In this study, we report a novel method of combining poly-aminoimide homopolymer with superparamagnetic core-shell nanoparticles and TRA as the template (MMIPNPs) for the extraction of TRA from solutions. The performance of this method is comparable with most of the analytical instrumental methods reported for TRA determination such as GC-MS [13,34–36] and HPLC [37–40].

2. Experimental

2.1. Reagents and materials

All the chemicals used were of analytical reagent grade or the highest purity available from Merck Company (Darmstadt, Germany). Double distilled water (DDW) was used throughout. All glassware were soaked in dilute nitric acid for 12 h and then thoroughly rinsed with DDW. The TRA stock solution was prepared weekly and stored at +4 °C. Working standard solutions of different TRA concentrations were prepared daily by diluting the stock solution.

2.2. Apparatus

The size, morphology and structure of the nanoparticles were characterized by transmission electronic microscopy (TEM, Philips, CM120, 100 kV). The crystal structure of the synthesized materials was determined by an X-ray diffractometer (XRD, 38066 Riva, d/G, Via M. Misone, 11/D (TN) Italy) at ambient temperature.

A Metrohm model 713 pH-meter was used for pH measurements. A single beam UV-mini-WPA spectrophotometer was used for the determination of TRA concentration in solutions. The mid-infrared spectra of Fe_3O_4, silica-coated magnetite nanoparticles (SiO_2–Fe_3O_4) and MMIPNPs in the region 4000–400 cm^{-1} were recorded by a FT-IR spectrometer (Perkin–Elmer model Spectrum GX) using KBr pellets. A 40 kHz universal ultrasonic cleaner water bath (RoHS, Korea) was used.

The magnetic properties of bare Fe_3O_4, Fe_3O_4–SiO_2 and MMIPNPs nanoparticles were measured with a vibrating sample magnetometer (VSM, 4 in. Daghigh Meghnatis Kashan Co., Kashan, Iran).

2.3. Preparation of nanostructured SiO_2–Fe_3O_4

The magnetite nanoparticles (Fe_3O_4) were prepared by the conventional co-precipitation method, with minor modifications [41]. $FeCl_3 \cdot 6\,H_2O$ (11.68 g) and $FeCl_2 \cdot 4\,H_2O$ (4.30 g) were dissolved in 200 mL DDW with vigorous stirring at 85 °C under nitrogen gas atmosphere. Then, 20 mL of 30% aqueous NH_3 was added to the solution. The color of the bulk solution changed from orange to black immediately. The magnetite precipitates were washed twice with DDW and once with 0.02 mol L^{-1} sodium chloride by magnetic decantation. Then, to the magnetite nanoparticles prepared above (0.8 g) was added an aqueous solution of tetraethoxy silane (TEOS, 10% (v/v), 80 mL), followed by glycerol (60 mL). The pH of the suspension was adjusted to 4.6 using glacial acetic acid, and the mixture was then stirred and heated at 90 °C for 2 h under nitrogen atmosphere. After cooling to room temperature, the suspension was washed sequentially with DDW (3 × 50 mL), methanol (3 × 50 mL), and DDW (5 × 50 mL).

2.4. Preparation of MIP and non-imprinted polymer (NIP)

The aminoimide monomer used for preparation of the poly-aminoimide homopolymer was synthesized according to a previously reported procedure [42]. Briefly, the aminoimide monomer was synthesized by slow addition of maleic anhydride (1 g) to the solution of ethylenediamine (1 mL) in DDW (20 mL). The solution was heated to 120 °C for 1 h, until all the water was removed and ethylenediamine reacted with maleic anhydride through ring opening. Then, the unsaturated aminoimide monomer was prepared by heating the reaction product to 140 °C for 2 h. In order to prepare MMIPNPs, the aminoimide monomer was homopolymerized in the presence of Fe_3O_4–SiO_2 (0.5 g), ammonium persulfate (0.1 g, as the initiator), ethylene glycol

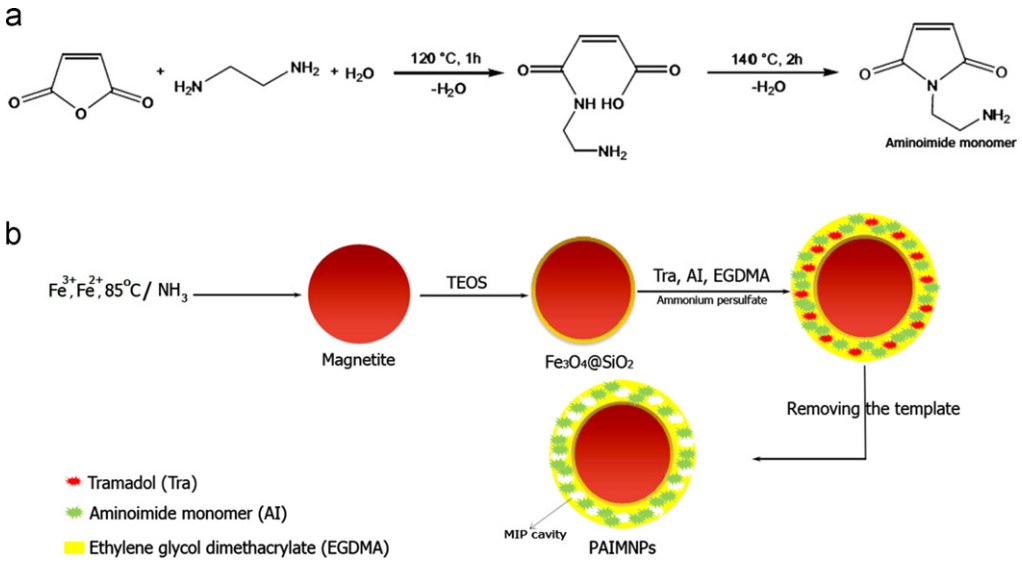

Scheme 1. Reaction involved in the synthesis of MMIPNPs.

dimethacrylate (2 mL, as the crosslinking monomer) and tramadol hydrochloride (0.01 g, as the template) in 30 mL DDW at 85 °C for 12 h according to Scheme 1. The product was separated by a magnet and washed overnight with a mixture of methanol:acetic acid (9:1, v/v) to remove the template. Finally, the product was washed with methanol to neutral pH and the resulting particles were dried under vacuum for 12 h. The NIP nanoparticles were also synthesized by the same procedure, without addition of the template (TRA).

2.5. Drug removal experiments

To a 20 mL sample solution containing TRA was added 0.1 g of MMIPNPs and its pH was adjusted to 7.0 with 0.1 mol L^{-1} HCl and/or 0.1 mol L^{-1} NaOH solution. The solution was shaken at room temperature for 25 min. Subsequently, the TRA loaded MMIPNPs were separated from the mixture with a permanent hand-held magnet within 60 s. The residual amount of the drug in solution was determined spectrophotometrically at the maximum absorbance wavelength of TRA (272 nm). The percent adsorption, i.e., the drug removal efficiency, was determined using the following equation:

$$\%R = \left[\frac{(C_0 - C_t)}{C_0}\right] \times 100 \quad (1)$$

where C_0 and C_t represent the initial and final (after adsorption) concentrations of the drug in mg L^{-1}, respectively. All the experiments were performed at room temperature.

2.6. Determination of TRA after preconcentration

Adsorption studies for determination of trace amounts of TRA were performed by adding 100.0 mL of solutions containing 3.0–200.0 ng mL^{-1} of TRA to 0.1 g MMIPNPs, the pH of which was adjusted at 7.0 using 0.1 mol L^{-1} HCl and/or 0.1 mol L^{-1} NaOH. Then the solutions were stirred for 25 min. The concentration of TRA decreased with time due to its adsorption by MMIPNPs. The TRA loaded nanoparticles were separated with magnetic decantation and desorption was performed with 1.0 mL of a methanol/acetic mixture (9:1 v/v). The concentration of TRA in the resulting solution was measured spectrophotometrically at 272 nm (λ_{max} of TRA).

2.7. Point of zero charge of the nanoparticles (pH_{pzc})

The point of zero charge (pzc) is a characteristic of metal oxides (hydroxides) and of fundamental importance in surface science. It is a concept relating to the phenomenon of adsorption and describes the condition when the electrical charge density on a surface is zero. The surface charge of MMIPNPs with hydroxyl and amino groups is largely dependent on the pH of the solution, the pH_{pzc} caused by the amphoteric behavior of hydroxylated surface groups, and the interaction between surface sites and the electrolyte species. When brought into contact with aqueous solutions, hydroxyl groups of surface sites can undergo protonation or deprotonation, depending on the solution pH, to form charged surface species. In this study, the pH_{pzc} of the MMIPNPs was determined in degassed 0.01 mol L^{-1} $NaNO_3$ solution at 20 °C. Aliquots of 30 mL of 0.01 mol L^{-1} $NaNO_3$ were mixed with 30 mg MMIPNPs in several beakers. The pH of the solutions were adjusted to 4.0, 5.0, 6.0, 7.0, 8.0, 9.0 and 10.0 using HNO_3 and/or NaOH solution, as appropriate. The initial pH values of the solutions were recorded, and the beakers were covered with parafilm and shaken for 24 h. The final pH values were recorded and the differences between the initial and the final pH (the so-called ΔpH) of the solutions was plotted against their initial pH values. The pH_{pzc} corresponds to the pH where ΔpH=0 [43].

2.8. Urine sample treatment

Urine samples were obtained from fasting healthy women. The samples were centrifuged for 10 min at 4000 rpm and filtered through a cellulose acetate filter (0.45-μm pore size, Millipore HA WP 04700). The filtrates were collected in glass containers which had been carefully cleaned with hydrochloric acid and washed with DDW, and stored at +4 °C until analysis was performed, with the minimum possible delay.

3. Results and discussion

3.1. Characterization of the adsorbent

The magnetization curves of the bare Fe_3O_4, Fe_3O_4–SiO_2 and MMIPNPs nanoparticles recorded with VSM are illustrated in Fig. 1. As shown in Fig. 1, the magnetization of the samples would approach the saturation values when the applied magnetic field increases to 10,000 Oe. The saturation magnetization of the bare Fe_3O_4 nanoparticles is 69.83 emu/g. For Fe_3O_4–SiO_2 and MMIPNPs nanoparticles, the saturation magnetizations are 54.83 and 53.13 emu/g, respectively. These results show that magnetic properties are hardly affected by the surface modification. A magnetization reduction of about 21.5% is observed between uncoated and SiO_2-coated Fe_3O_4 nanaoparticles, and about 3.10% between Fe_3O_4–SiO_2 and its polymer-coated form (MMIPNPs). This may be related to the nanoparticle size effect, the increased surface disorder, and the diamagnetic contributions of SiO_2 and polymer layers. The amount of decrease is not that large to seriously affect the use of these nanoparticles for the desired application.

The FT-IR spectra of the products in each step of the MMIPNPs synthesis were recorded to verify the formation of the expected products. The related spectra are shown in Fig. 2. The characteristic absorption band of Fe–O in Fe_3O_4 (around 580 cm^{-1}) is observed in Fig. 2a. A strong peak at 1064 cm^{-1} in Fig. 2b is attributed to Si–O in SiO_2. Two new absorption peaks at 1729.3 cm^{-1} and 1440 cm^{-1} in Fig. 2c are assigned to C=O and C–N bands in the polymer-coated final product (MMIPNPs), respectively. Moreover, new absorption peaks at 3248.61 and 3071.9 cm^{-1} are related to the stretching modes of the amino group (N–H) [41]. Based on the above results, it can be concluded

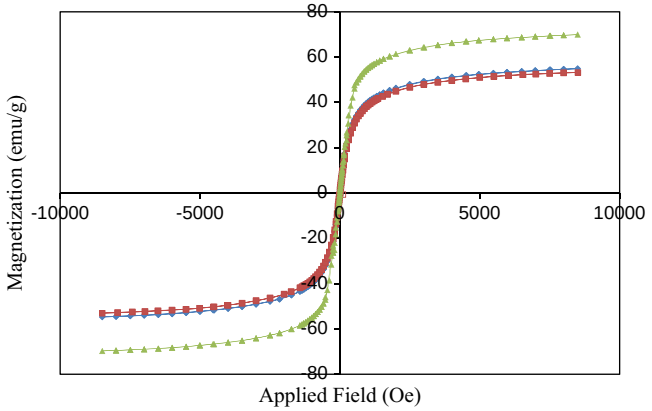

Fig. 1. Magnetization curves obtained by vibrating sample magnetometer (VSM) at room temperature: (▲) bare Fe_3O_4; (◆) Fe_3O_4–SiO_2; and (■) MMIPNPs nanoparticles.

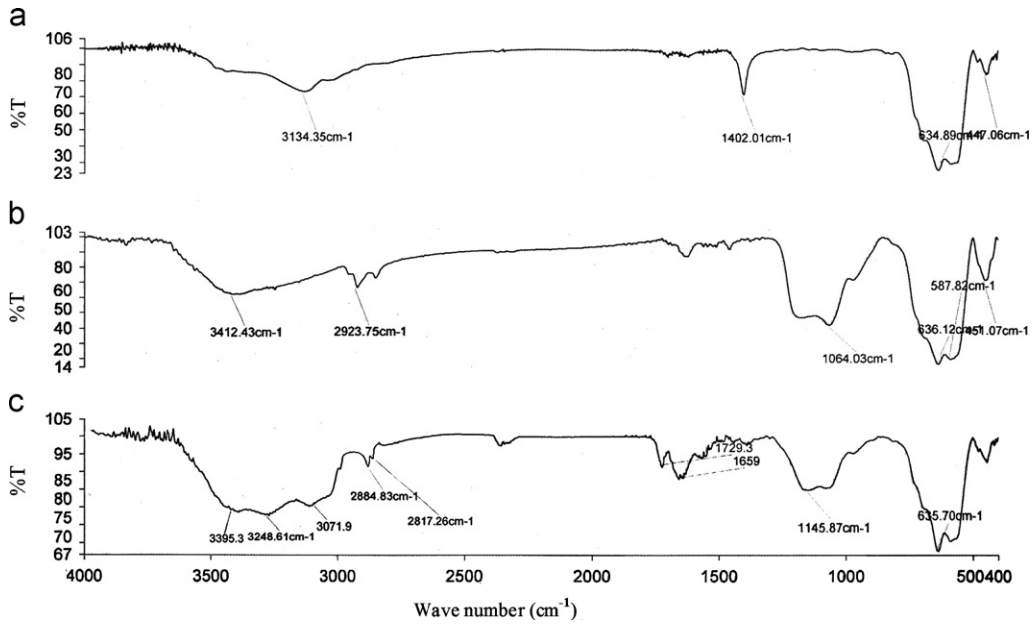

Fig. 2. FT-IR spectra of (a) Fe_3O_4, (b) SiO_2–Fe_3O_4 and (c) MMIPNPs.

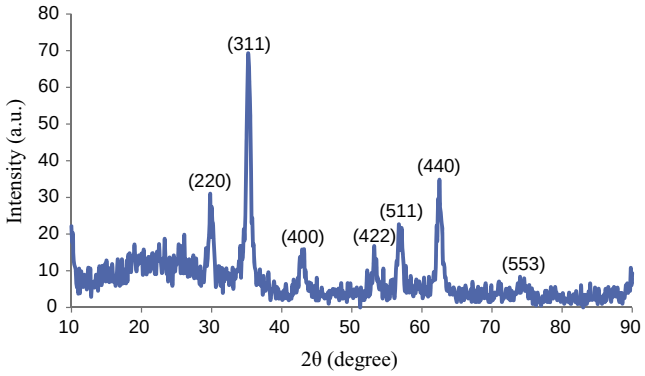

Fig. 3. XRD patterns of MMIPNPs.

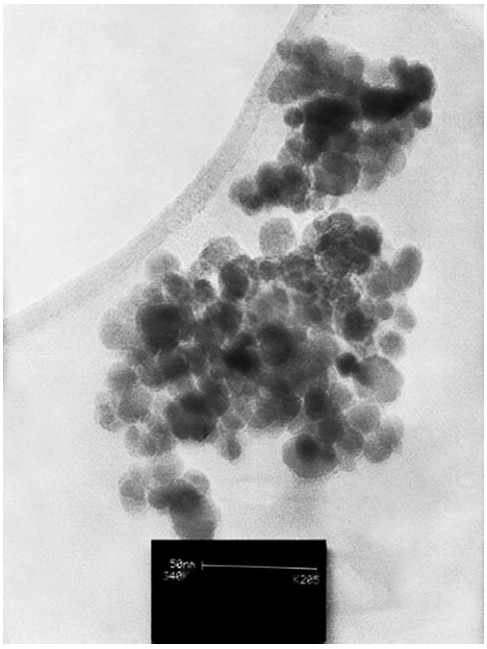

Fig. 4. TEM images of MMIPNPs.

that the fabrication procedure (in Section 2.4) has been successfully performed.

The XRD pattern (Fig. 3) shows diffraction peaks that are indexed to (220), (311), (400), (422), (511), (440) and (553) reflections characteristic of the cubic spinel phase of Fe_3O_4 (JCPDS powder diffraction data file no. 79-0418), revealing that the resultant nanoparticles are mostly Fe_3O_4. The average crystallite size of the Fe_3O_4 nanoparticles was estimated to be 12 nm from the XRD data according to the Scherrer equation.

The TEM image of the MMIPNPs in Fig. 4 indicates that the Fe_3O_4 nanoparticles are enwrapped rather homogeneously in SiO_2 shells, and further by an MIP layer. The average size of the synthesized nanoparticles is estimated to be about 25 nm.

3.2. Effect of initial solution pH on the TRA uptake

Solution pH affects the adsorption process of drug molecules by affecting both aqueous chemistry and surface binding-sites of the adsorbent. The effect of pH on the TRA removal was investigated in the range 3.0–9.0 using an initial TRA concentration of 20.0 mg L^{-1} and a stirring time of 45 min, where the pH was adjusted with 0.1 mol L^{-1} HCl and/or NaOH solutions. Fig. 5 shows the amount of TRA adsorbed per gram of adsorbent (q_e) as a function of pH, indicating that the adsorbent provides highest affinity to TRA at pH 7.0. This is reasonable, because both the adsorbent and the analyte are neutral at this pH (pH_{pzc} of MMIPNPs is 7.0, Fig. 6, and pK_a of TRA is 9.3 [44]), and hence, the highest non electrostatic interaction between TRA and MMIPNPs is expected at this pH.

3.3. Effect of adsorbent dosage on the drug adsorption

The adsorbent dosage is an important parameter in adsorption studies, because it determines the capacity of the adsorbent for a given initial concentration of drug solution. The adsorption percentage is increased with increase in the dosage of MMIPNPs; however, the adsorption capacity dropped with increasing the MMIPNPs dosage. In fact, increasing the MMIPNPs dosage increases the probability of the MMIPNPs entanglement in solution, causing adsorption in the interlayer space, and a decrease in

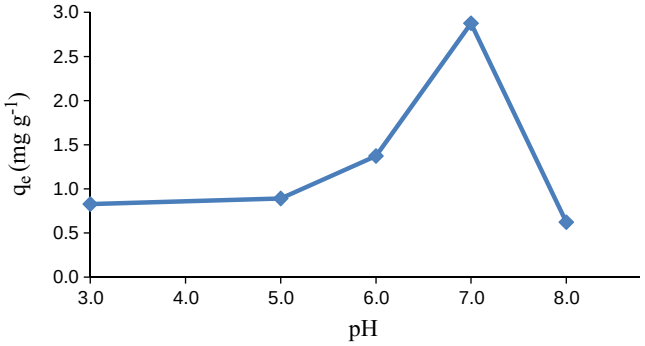

Fig. 5. Amount of TRA uptake per gram of adsorbent at different pH values.

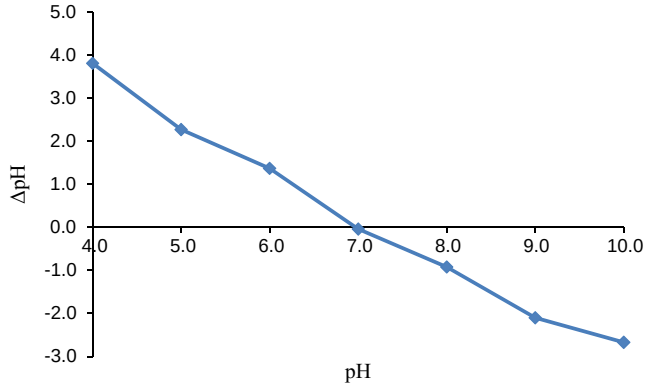

Fig. 6. Point of zero charge (pH_{pzc}) of MMIPNPs.

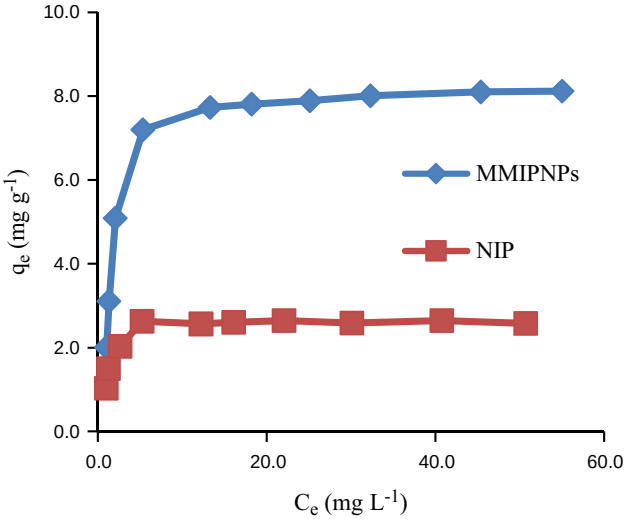

Fig. 7. Isothermal adsorption curves of TRA on MMIPNPs (◆) and on NIP nanoparticles (■).

Table 1
Adsorption isotherm parameters for Langmuir and Freundlich models.

Isotherm model	Langmuir			Freundlich		
Parameters	K_L	q_m (mg g^{-1})	R^2	K_F	$1/n$	R^2
MMIPNPs	4.77	8.51	0.9989	3.09	0.28	0.767
NIPNPs	1.57	2.65	0.9990	1.44	0.19	0.707

the aggregation of the drug at the external surface. Accordingly, the adsorption capacity declined as the MMIPNPs dosage increased. Moreover, high MMIPNPs dosage may influence the physical characteristics of the solid–liquid suspension, for example, by increasing the viscosity and inhibiting the diffusion of the drug molecules to the surface of the MMIPNPs. Since the initial concentration of TRA was fixed, the decrease in the adsorption capacity by increasing the MMIPNPs dosage can be related to the availability of more surface area of the MMIPNPs [43].

3.4. Effect of contact time

The effect of contact time on the adsorption of drug was studied to determine the time needed to remove TRA by MMIPNPs from a 20.0 mg L^{-1} solution of the drug at pH 7.0. A 0.1 g of the adsorbent was added into 20 mL of the drug solution. Absorbance of the solution at λ_{max} of TRA was monitored vs. time to determine variation of the drug concentration. It was observed that after a contact time of about 25 min, almost all the drug was adsorbed.

3.5. Adsorption isotherms

The capacity of the adsorbent is an important factor that determines how much sorbent is required to quantitatively remove a specific amount of the drug from solution. For measuring the adsorption capacity of MMIPNPs, the absorbent was added into TRA solutions at various concentrations, and the suspensions were stirred at room temperature, followed by magnetic removal of the absorbent. An adsorption isotherm describes the fraction of the sorbate molecules that are partitioned between the liquid and the solid phase at equilibrium. Adsorption of the drug by MIP and NIP nanoparticles was modeled using Freundlich [45] and Langmuir [46] adsorption isotherms. The remained TRA in the supernatants were measured spectrophotometrically, and the results were used to plot the isothermal adsorption curves as shown in Fig. 7. The equilibrium adsorption data were fitted to Langmuir and Freundlich isotherm models by linear regression. The resulting parameters are summarized in Table 1.

The higher correlation coefficient obtained for the Langmuir model ($R^2 > 0.99$) indicates that the experimental data are better fitted into this model, and adsorption of TRA on MMIPNPs is more compatible with Langmuir assumptions, i.e., adsorption takes place at specific homogeneous sites within the adsorbent. The Langmuir model is based on the physical hypothesis that the maximum adsorption capacity consists of a monolayer adsorption, that there is no interaction between adsorbed molecules, and that the adsorption energy is distributed homogeneously over the entire coverage surface. This sorption model serves to estimate the maximum uptake values where they cannot be reached in the experiments. According to the results (Table 1), the maximum amount of TRA that can be adsorbed by MMIPNPs was found to be 8.51 mg g^{-1} at pH 7.0. The relatively high adsorption capacity of MMIPNPs shows that the adsorption of TRA molecules takes place at a large number of specific homogeneous sites within the adsorbent (specific cavities of the MIP), besides non-specific interactions which are approximately identical for both MMIPNPs and NIP nanoparticles.

3.6. Reusability and stability

The reusability and stability of MMIPNPs for the extraction of TRA was assessed by performing five consecutive separation/desorption cycles under the optimized conditions. The desorption of TRA from the adsorbent was performed with methanol/acetic acid mixture as described in Section 2.6. There was no significant change in the performance of the adsorbent during these cycles,

Table 2
Assay of TRA in human urine samples by means of the proposed method ($N=5$).

Sample	Spiked value ($ng\,mL^{-1}$)	Found ($ng\,mL^{-1}$)	Recovery percent
Human urine	–	0.00 ± 0.01	–
	10	9.82 ± 0.03	98.2
	20	20.03 ± 0.01	100.1
Infected human urine	–	115.23 ± 1.07	–
	10	124.86 ± 1.15	96.1
	20	135.12 ± 0.85	99.5

Table 3
Comparison of the proposed method with other reported methods for TRA determination.

Method	Sample	LOD ($ng\,mL^{-1}$)	Ref.
[a]HF-LPME/GC-MS	Plasma and urine	0.08	[13]
[b]HS-SPME/GC-MS	Plasma	0.2	[34]
LLE/GC-MS	Plasma	3.45	[35]
SPE–GC-MS	Hair	10	[36]
[c]LPME-BE/HPLC	Plasma and urine	0.12	[37]
SPE/HPLC	Plasma	50	[38]
LLE–HPLC	Plasma	10	[39]
LLE/HPLC	Plasma	2.5	[40]
MMIPNPs	Urine	1.5	Proposed method

[a] Hollow-fiber liquid phase micro extraction.
[b] Head space-solid phase micro extraction
[c] Liquid phase micro extraction-back extraction.

indicating that the fabricated MMIPNPs is a reusable and stable solid phase sorbent for the extraction of TRA.

3.7. Effect of sample volume

The effect of sample volume on the drug adsorption was studied in the range 10.0–200.0 mL; 10.0 mL samples containing 20.0 $mg\,L^{-1}$ of the drug were diluted to 20.0, 25.0, 50.0, 75.0, 100.0, 125.0, 150.0 and 200.0 mL with DDW. Then adsorption and desorption processes were performed under the optimum conditions (pH 7.0; contact time, 25 min; MMIPNPs dosage, 0.1 g) as described in the experimental section. The results showed that the drug content in the volumes up to 100.0 mL was completely and quantitatively adsorbed by the nanoparticles, but there was a decrease in the amount adsorbed at higher volumes. Therefore, for the determination of trace quantities of the drug, a sample volume of 100.0 mL was selected for a high preconcentration factor.

3.8. Analytical parameters and applications

Calibration graph was constructed from spectrophotometric measurement of the desorbed TRA after performing its adsorption/separation under the optimum conditions described above. The calibration graph was linear in the range 3.0–200.0 $ng\,mL^{-1}$ for a sample volume of 100.0 mL. The calibration equation is $A=0.010C+0.0060$ with a correlation coefficient of 0.9968 ($n=10$), where A is the absorbance of the eluate at 272 nm and C is concentration of the drug in $ng\,mL^{-1}$. The limit of detection, defined as $LOD=3S_b/m$, (where LOD, S_b and m are the limit of detection, standard deviation of the blank and the slope of the calibration graph, respectively), was 1.5 $ng\,mL^{-1}$ of TRA. As the drug in 100.0 mL of the sample solution was concentrated into 1.0 mL, a preconcentration factor of 100.0 was achieved in this method.

The analytical applicability of the proposed method was evaluated by determining the TRA content of infected and healthy human urine samples. The samples were also analyzed after spiking with different amounts of the drug. The relative standard deviations (RSD) for 20.0 and 50.0 $ng\,mL^{-1}$ of the drug were 1.26% and 0.83% ($n=5$), respectively. The results given in Table 2 show good recoveries of the proposed method for the TRA added to urine samples.

Table 3 shows a comparison of the results of the present method with several other methods reported for the determination of TRA. It should be highlighted that the major advantages of the magnetic separation with MMIPNPs are easy separation and reversibility of the process, i.e., the adsorbent is easily attracted by a magnet and can be separated from the liquid medium, the drug can be recovered from the nanoparticles and the regenerated nanoparticles can be reused for further drug removal. Table 3 shows that the LOD of the proposed method is comparable with those based on GC-MS and HPLC analysis.

4. Conclusions

In this paper, novel superparamagnetic surface molecularly imprinted nanoparticles were prepared using a synthesized monomer. The synthesized MMIPNPs showed higher molecular recognition than the NIP. Based on MMIPNPs, a solid phase extraction-UV–vis method has been developed for the separation of TRA from aqueous solutions. The adsorbent is easily attracted by a magnet and can be separated from the liquid medium which enables an easy separation process. Furthermore, the MIP nanoparticles as a new sorbent in solid phase extraction were successfully investigated for the clean-up of human urine samples with an optimized procedure. The method was applied to the trace TRA determination in healthy and infected human urine samples. The recoveries of TRA spiked into human urine samples were in the range 96.1–100.1%. The statistical parameters and the recovery study data clearly indicate reproducibility and accuracy of the proposed method.

References

[1] F. Musshoff, B. Madea, Forensic Sci. Int. 116 (2001) 197–199.
[2] C.R. Lee, D. Mc Tavish, E.M. Sorkin, Drugs 46 (1993) 313–340.
[3] R.B. Raffa, E. Friderichs, W. Reimann, R.P. Shank, E.E. Codd, J.L. Vaught, J. Pharmacol. Exp. Ther. 260 (1992) 275–285.
[4] K.S. Lewis, N.H. Han, Am. J. Health Syst. Pharm. 54 (1997) 643–652.
[5] W. Lintz, H. Barth, R. Becker, E. Frankus, E. Schmidt-Bothelt, Arzneimittelforschung 48 (1998) 436–447.
[6] L. Qu, S. Feng, Y. Wu, Y. Wu, Sichuan Da Xue Xue Bao Yi Xue Ban J. Sichuan University. Med. Sci. Ed. 34 (2003) 574–575.
[7] G.C. Yeh, M.T. Sheu, C.L. Yen, Y.W Wang, C.H. Liu, H.O. Ho, J. Chromatogr. B 723 (1999) 247–253.
[8] S.H. Gan, R. Ismail, W.A.W. Adnan, Z. Wan, J. Chromatogr. B 772 (2002) 123–129.
[9] M. Nobilis, J. Pastera, P. Anzenbacher, D. Svoboda, J. Kopecky, F. Perlik, J. Chromatogr. B 681 (1996) 177–183.
[10] H. Ebrahimzadeh, Y. Tamini, A. Sedighi, M.R. Rouini, J. Chromatogr. B 863 (2008) 229–234.
[11] A. Kucuk, Y. Kadioglu, F. Celebi, J. Chromatogr. B 816 (2005) 203–208.
[12] S.T. Ho, J.J. Wang, W.J. Liaw, C.M. Ho, J.H. Li, J. Chromatogr. B 736 (1999) 89–96.
[13] M. Ghambarian, Y. Yamini, A. Esrafili, J. Pharm. Biomed. Anal. 56 (2011) 1041–1045.
[14] M. Merslavic, L.Z. Kralj, J. Chromatogr. B 693 (1997) 222–227.
[15] V. Gambaro, C. Benvenuti, L.D. Ferrari, L.D. Acqua, F. Fare II, Farmaco 58 (2003) 947–950.
[16] H.J. Leis, G. Fauler, W. Windischhofer, J. Chromatogr. B 804 (2004) 369–374.
[17] Y.F. Sha, S. Shen, G.L. Duan, J. Pharm. Biomed. Anal. 37 (2005) 143–147.
[18] Q. Tao, D.J. Stone Jr., M.R. Borenstein, V. Jean-Bart, E.E. Codd, T.P. Coogan, D.D. Krieger, S. Liao, R.B. Raffa, J. Chromatogr. B 763 (2001) 165–171.
[19] Y.H. Ardakani, M.R. Rouini, J. Pharm. Biomed. Anal. 44 (2007) 1168–1173.
[20] L. Qin, W. Rui, Chin. Med. J. 119 (2006) 2013–2021.

[21] L.M. Zhao, X.Y. Chen, J.J. Cui, M. Sunita, D.F. Zhong, Yao Xue Xue Bao, Acta Pharmaceutica Sinica 39 (2004) 458–462.
[22] A. Ceccato, P. Chiap, P. Hubert, J. Crommen, J. Chromatogr. B 698 (1997) 161–170.
[23] L. Vlase, S.E. Leucuta, S. Imre, Talanta 75 (2008) 1104–1109.
[24] M. Javanbakht, A.M. Attaran, M.H. Namjumanesh, M. Esfandyari-Manesh, B. Akbari-adergani, J. Chromatogr. B 878 (2010) 1700–1706.
[25] M.-C. Hennion, J. Chromatogr. A 856 (1999) 3–54.
[26] C. He, Y. Long, J. Pan, K. Li, F. Liu, J. Biochem. Biophys. Methods 70 (2007) 133–150.
[27] B. Sellergren (Ed.), Molecularly Imprinted Polymers: Man-Made Mimics of Antibodies and Their Applications in Analytical Chemistry (Techniques and Instrumentation in Analytical Chemistry), vol. 23, Elsevier, Amsterdam, 2001.
[28] Y. Li, X. Li, J. Chu, C. Dong, J. Qi, Y. Yuan, Environ. Pollut. 158 (2010) 2317–2323.
[29] Z. Lin, W. Cheng, Y. Li, Z. Liu, X. Chen, C. Huang, Anal. Chim. Acta 720 (2012) 71–76.
[30] N. Masque, R.M. Marce, F. Borrull, Trends Anal. Chem. 20 (2001) 477–486.
[31] M. Walshe, J. Howarth, M.T. Kelly, R. O'Kennedy, M.R. Smyth, J. Pharm. Biomed. Anal. 16 (1997) 319–325.
[32] A. Zander, P. Findlay, T. Renner, B. Sellergren, A. Swietlow, Anal. Chem. 70 (1998) 3304–3314.
[33] L.I. Andersson, A. Paprica, T. Arvidsson, Chromatographia 46 (1997) 57–62.
[34] Y.F. Sha, S. Shen, G.L. Duan, J. Pharm. Biomed. Anal. 37 (2005) 143–147.
[35] H.J. Leis, G. Fauler, W. Windischhofer, J. Chromatogr. B 804 (2004) 369–374.
[36] C. Moore, S. Rana, C. Coulter, J. Chromatogr. B 850 (2007) 370–375.
[37] H. Ebrahimzadeh, Y. Yamini, A. Sedighi, M.R. Rouini, J. Chromatogr. B 863 (2008) 229–234.
[38] S.H. Gan, R. Ismail, J. Chromatogr. B Biomed. Sci. Appl. 759 (2001) 325–335.
[39] S.H. Gan, R. Ismail, W.A. Wan Adnan, Z. Wan, J. Chromatogr. B 772 (2002) 123–129.
[40] M.R. Rouini, Y.H. Ardakani, F. Soltani, H.Y. Aboul-Enein, A. Foroumadi, J. Chromatogr. B 830 (2006) 207–211.
[41] T. Madrakian, A. Afkhami, M.A. Zolfigol, M. Ahmadi, N. Koukabi, Nano-Micro Lett. 4 (2012) 57–63.
[42] N.M. Mahmoodi, F. Najafi, S. Khorramfar, F. Amini, M. Arami, J. Hazard. Mater. 198 (2011) 87–94.
[43] T. Madrakian, A. Afkhami, M. Ahmadi, H. Bagheri, J. Hazard. Mater. 196 (2011) 109–114.
[44] M.N. Aamir, M. Ahmad, N. Akhtar, G. Murtaza, S.A. Khan, S. Zaman, A. Nokhodchi, Int. J. Pharm. 407 (2011) 38–43.
[45] H. Freundlich, W. Heller, J. Am. Chem. Soc. 61 (1939) 2228–2230.
[46] I. Langmuir, J. Am. Chem. Soc. 38 (1916) 2221–2295.